

Multi-objective optimization-based method for kinematic posture prediction: development and validation

Jingzhou (James) Yang^{†*}, Tim Marler[‡] and Salam Rahmatalla[‡]

[†]*Department of Mechanical Engineering, Texas Tech University, Lubbock, TX 79409, USA*

[‡]*Center for Computer-Aided Design, The University of Iowa, Iowa City, IA 52242, USA*

(Received in Final Form: February 19, 2010. First published online: April 30, 2010)

SUMMARY

Posture prediction plays an important role in product design and manufacturing. There is a need to develop a more efficient method for predicting realistic human posture. This paper presents a method based on multi-objective optimization (MOO) for kinematic posture prediction and experimental validation. The predicted posture is formulated as a multi-objective optimization problem. The hypothesis is that human performance measures (cost functions) govern how humans move. Twelve subjects, divided into four groups according to different percentiles, participated in the experiment. Four realistic in-vehicle tasks requiring both simple and complex functionality of the human simulations were chosen. The subjects were asked to reach the four target points, and the joint centers for the wrist, elbow, and shoulder and the joint angle of the elbow were recorded using a motion capture system. We used these data to validate our model. The validation criteria comprise R-square and confidence intervals. Various physics factors were included in human performance measures. The weighted sum of different human performance measures was used as the objective function for posture prediction. A two-domain approach was also investigated to validate the simulated postures. The coefficients of determinant for both within-percentiles and cross-percentiles are larger than 0.70. The MOO-based approach can predict realistic upper body postures in real time and can easily incorporate different scenarios in the formulation. This validated method can be deployed in the digital human package as a design tool.

KEYWORDS: Digital humans; Predicted posture; MOO; Human performance measures; Validation.

1. Introduction

Posture prediction is an important component within the human modeling and simulation package. Posture prediction aims to predict a static single posture for a specific scenario. Motion prediction is a dynamic problem that aims to predict time-dependent postures for a given period. Posture prediction is the foundation for understanding motion prediction, so that is what we focus on in this work.

The objective of this work is to develop a MOO-based kinematic upper body posture prediction model and validate this model using experiments. In this paper, we present the

details of the MOO model, the experimental protocol, criteria for validation, and a two-domain validation method.

There are three types of approaches for posture prediction. The first is an experiment-based method (empirical–statistical approach) in which the posture comes from experiments and statistic regression. The second is a direct inverse kinematic method, and the third is a direct optimization-based method.

In the empirical–statistical approach, data are collected either from thousands of experiments with human subjects or from simulations with three-dimensional computer-aided human-modeling software.^{6,26} The data are then analyzed statistically in order to form predictive posture models. These models have been implemented in the simulation software along with various methods for selecting the most probable posture given a specific scenario.^{1,5,8}

The direct inverse kinematics approach to posture prediction has received substantial attention. With this approach, the position of a limb is modeled mathematically with the goal of formulating a set of equations that provide the joint variables.^{13,14,15,16,29–31} Griffin¹⁰ gives a review of the validation of biodynamic models. Wang *et al.*³² demonstrate the validation of the model-based motion in the REALMAN project.

The direct optimization-based method considers posture prediction an optimization problem in which humans choose a posture to minimize certain objective functions.^{18,19,33,36,37} In the biomechanics literature, significant efforts have focused on static lifting posture prediction in three different behavioral criteria or objective functions. The first criterion assumes that subjects choose a posture that requires the minimum overall effort.³ The second criterion assumes that subjects minimize local effort or fatigue.^{2,24} The third criterion assumes that subjects choose the posture with the greatest stability.¹⁷ Dysart and Woldstad⁷ compared these three models. This paper presents the development and validation of the MOO-based kinematic posture prediction model based on our previous work).^{18,19,33,36,37}

This paper is organized as follows: Section 2 introduces the MOO-based posture prediction model, Section 3 presents the detailed validation process, and Section 4 presents the conclusion and discussion.

2. MOO-based Method for Kinematic Posture Prediction

In this section, we briefly introduce the kinematic model for a digital human model, derive human performance measures,

* Corresponding author. Email: james.yang@ttu.edu

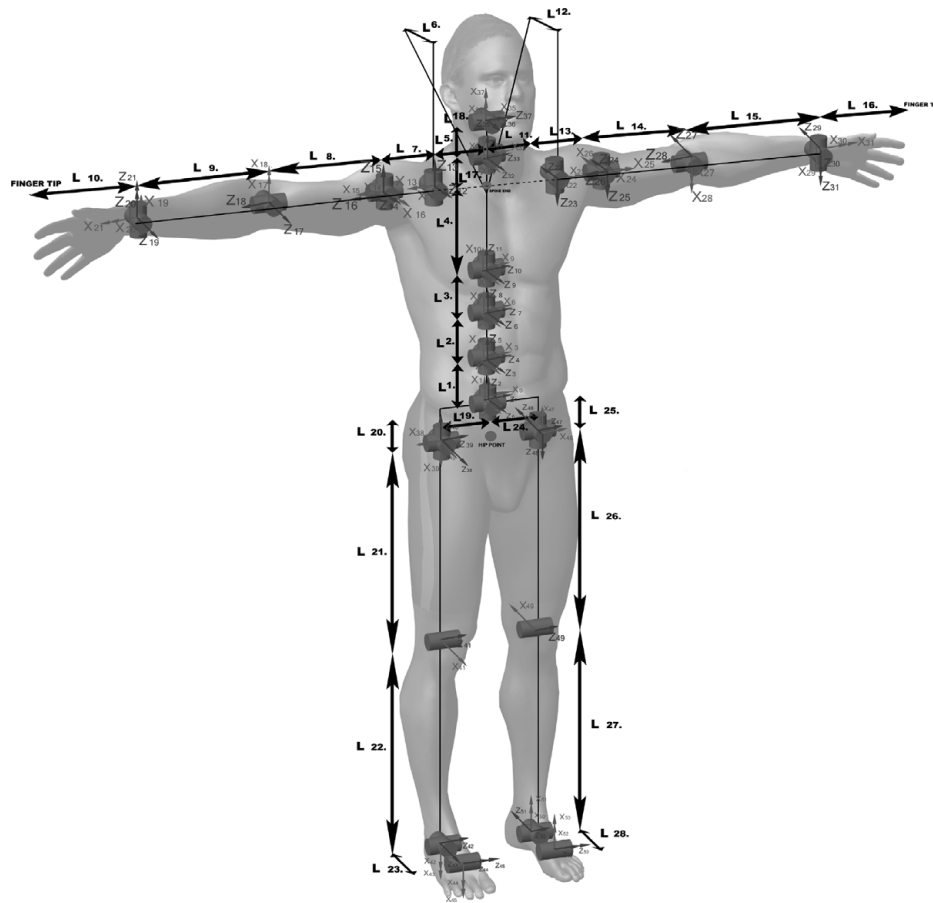


Fig. 1. Kinematic model.

and formulate the redundant inverse kinematics problem as a MOO problem.

We have developed a digital human with 109 degrees of freedom (DOFs),^{34,36} shown in Fig. 1 based on Denavit Hartenberg method.⁴ In this model, the kinematic joints from the waist to the right hand have 21 DOFs and are represented by q_1, \dots, q_{21} , respectively. The kinematic joints from the left clavicle to the left hand have 9 DOFs and are described by q_{22}, \dots, q_{30} . The kinematic joints for the neck have 5 DOFs and are denoted by q_{31}, \dots, q_{35} . Joints for legs and feet are represented by q_{36}, \dots, q_{49} . Each eye has 2 DOFs, each hand has 25 DOFs,²⁵ and the model has 6 global DOFs (3 prismatic and 3 rotational joints). It has five open loops starting from the root at the hip point to the right hand, left hand, head, left leg, and right leg.

Posture prediction is defined as follows. We try to find the configuration (joint angles \mathbf{q}) of a human when he or she reaches for a target point using the fingertip or other end-effector (point of interest on body). Because the human model has a high number of DOFs, this problem is a redundant problem. The hypothesis is that human performance measures govern how humans move. An MOO-based optimization model is used to solve this problem.

Postures/motions inherit variability due to (1) various tasks and (2) variable anthropometry. Many human performance measures act together to govern human postures. In this study, one of the objectives is to develop the corresponding mathematical model (human performance measures). The first is that human posture gravitates to a “neutral posture,”

and there are different task-related neutral postures.¹⁴ For example, when humans stand to achieve a task, the neutral posture is one in which the arms are straight down at the sides, and the neck, torso, and legs remain straight in the frontal plane. When humans sit, the neutral position is one in which the torso leans on the seat back, knees bend, feet rest on the floor, and arms are on the arm rests of the seat. The second performance measure is potential energy.³³ Humans use one posture instead of another to save energy. For example, humans use the arm before the torso or clavicle because the mass of the arm is much smaller than the mass of the torso (this is obtained through observations). The third is that joints with tendons try to avoid stretching those tendons.²⁰ The fourth factor is vision;²¹ humans try to see a target as they reach for it. However, in the muscular discomfort function, joint displacement has been included in each joint. Therefore, three human performance measures are used as the cost function in the proposed method.

Based on human performance measures such as change of potential energy, visual displacement, and muscular discomfort,^{19,23,33,36} the MOO problem is formulated as follows:

$$\text{Find : } \mathbf{q} \in R^{DOF} \quad (1)$$

to minimize:

$$f(\mathbf{q}) = w_1 f_{Mus_discomfort}(\mathbf{q}) + w_2 f_{VisualDisplacement}(\mathbf{q}) + w_3 f_{delta_PE}(\mathbf{q})$$

subject to:

$$\text{distance} = \|\mathbf{x}(\mathbf{q})^{\text{end-effector}} - \mathbf{x}^{\text{target point}}\| \leq \varepsilon$$

$$q_i^L \leq q_i \leq q_i^U; i = 1, 2, \dots, DOF,$$

where w_i are the weights; ε is a small number that approximates zero; $\mathbf{x}(\mathbf{q})^{\text{end-effector}} \in R^3$ is the position vector in Cartesian space that describes the location of the end-effector as a function of the joint angles, with respect to the global coordinate system; and $\mathbf{x}(\mathbf{q})^{\text{target point}}$ is the position vector of the target point. All optimization problems are solved using the software SNOPT,⁹ which uses sequential quadratic programming. Analytical gradients are provided for all of the objective functions and for the constraint.

Three human performance measures have been developed and are defined in the following section:

2.1. Muscular discomfort

This function incorporates three facets of musculoskeletal discomfort: (1) the tendency to move toward a generally comfortable position, (2) the tendency to avoid postures in which joint angles are pushed to their limits, and (3) the idea that people strive to reach or contact a point using one set of body parts at a time. With regard to facet 2, the avoidance of joint limits does not apply to joints where ligaments and/or tendons are not stretched, as with the elbow and clavicle. With regard to facet 3, in terms of upper-body motion, one first tries to reach a point using one's arm. If that is unsuccessful, then one bends the torso. Finally, if necessary, the clavicle is extended. The intent in developing this performance measure is not to quantify discomfort but to model components that are proportional to discomfort. Consequently, only its relative values (from one posture to another), not its absolute values, are significant.

The final function is given as follows:

$$f_{\text{Mus_discomfort}}(\mathbf{q}) = \sum_{i=1}^{DOF} [\gamma_i (\Delta q_i^{\text{norm}}) + QU_i + QL_i], \quad (2)$$

where $\Delta q^{\text{norm}} = \frac{q_i - q_i^N}{q_i^U - q_i^L}$. QU and QL are specially designed penalty functions that incorporate the discomfort associated with joint angles that approach joint limits. They are defined as follows:

$$QU = \left(0.5 \sin \left(\frac{5.0 (q_i^U - q_i)}{q_i^U - q_i^L} + 1.571 \right) + 1 \right)^{100}, \quad (3)$$

$$QL = \left(0.5 \sin \left(\frac{5.0 (q_i - q_i^L)}{q_i^U - q_i^L} + 1.571 \right) + 1 \right)^{100}. \quad (4)$$

QU is zero until a joint angle is in the upper 5% of its range, and QL is zero until a joint angle is within the lower 5% of its range. γ_i represents weights, but these weights are not used in the same way that weights for joint displacement are. Instead, these are used to model the tendency to move different sets of body parts sequentially. The specific values for these weights are irrelevant; the weights simply need to

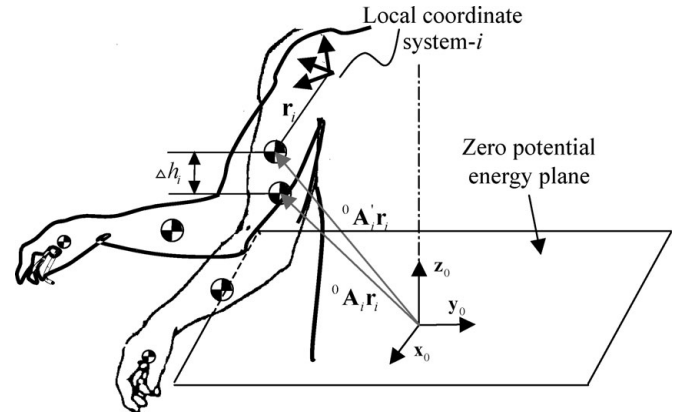


Fig. 2. Illustration of the potential energy of the forearm.

have significantly different orders of magnitude. The weights for the arms are equal to 1. The weights for the spine and neck DOFs are all 1×10^4 . The weights for the clavicle DOFs are 1×10^8 . Note that this assumption is only for static postures.

2.2. Delta potential energy

This function represents the change in potential energy (called delta potential energy) and uses weights that are based on the mass of different segments of the body. With this performance measure, the primary segments of the upper body are represented with six lumped masses: three for the lower, middle, and upper torso; one for the upper arm; one for the forearm; and one for the hand. Based on the definition of potential energy, the heights of the masses provide the components of the human performance measure. Then, mathematically, the weight (force of gravity) of a body segment provides a multiplier for movement of that segment in the vertical direction. In order to avoid having the virtual human constantly bend over and thus minimize potential energy, we actually minimize the *change* in potential energy. This means that each body segment essentially has a different datum, where the potential is assumed to be zero. The vector from the origin of a link's local coordinate system to its center of mass is given by ${}^i\mathbf{r}_i$, where the subscript indicates the relevant local coordinate system. In order to determine the position and orientation of any part of the body, we use the transformation matrices ${}^{(i-1)}\mathbf{A}_i$, which are 4×4 matrices that relate the local coordinate system i to the local coordinate system $i - 1$. Consequently, \mathbf{r}_i is actually an augmented 4×1 vector with respect to local coordinate system i , rather than a 3×1 vector typically used with Cartesian space. $\mathbf{g} = [0 -g \ 0 \ 0]^T$ is the augmented gravity vector. When the human upper body moves from one configuration to another, there are two potential energies: P'_i , which is associated with the initial configuration, and P_i , which is associated with the current configuration. Therefore, for the first body part in the chain (the lower torso), the potential energies are $P'_1 = m_1 \mathbf{g}^T {}^0\mathbf{A}'_1 \mathbf{r}_1$ and $P_1 = m_1 \mathbf{g}^T {}^0\mathbf{A}_1 \mathbf{r}_1$. The potential energies for the second body part are $P'_2 = m_2 \mathbf{g}^T {}^0\mathbf{A}'_1 {}^1\mathbf{A}'_2 \mathbf{r}_2$ and $P_2 = m_2 \mathbf{g}^T {}^0\mathbf{A}_1 {}^1\mathbf{A}_2 \mathbf{r}_2 + P_1$. The potential energies for the i th body part are $P'_i = m_i \mathbf{g}^T {}^0\mathbf{A}'_1 {}^1\mathbf{A}'_2 \dots {}^{(i-1)}\mathbf{A}'_i \mathbf{r}_i$ and $P_i = m_i \mathbf{g}^T {}^0\mathbf{A}_1 {}^1\mathbf{A}_2 \dots {}^{(i-1)}\mathbf{A}_i \mathbf{r}_i + P_{i-1}$. In Fig. 2, Δh_i is the y-component of the

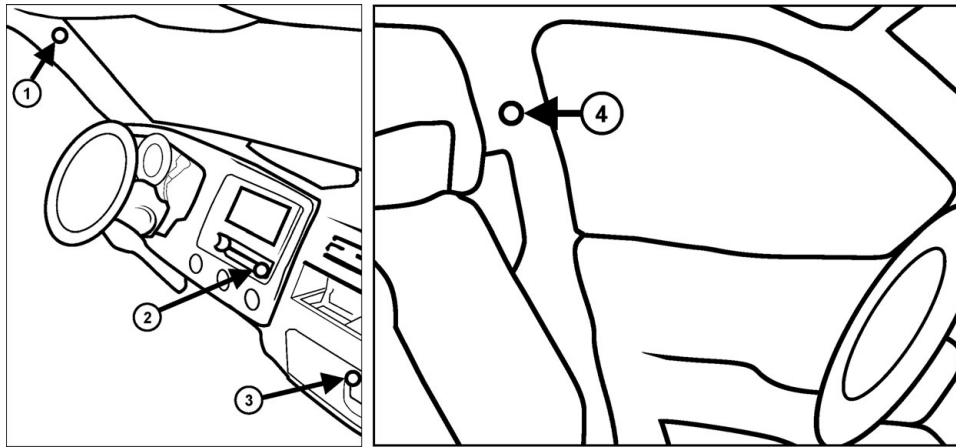


Fig. 3. Four in-vehicle tasks.

vector ${}^0\mathbf{A}'_1 \dots {}^{i-1}\mathbf{A}'_i \mathbf{r}_i - {}^0\mathbf{A}_1 \dots {}^{i-1}\mathbf{A}_i \mathbf{r}_i$. The final objective function, which is minimized, is defined as follows:

$$f_{Delta-PE}(\mathbf{q}) = \sum_{i=1}^{\kappa} (P_i - P'_i)^2. \quad (5)$$

Note that Eq. (6) can be written in the form of a weighted sum as follows:

$$f_{Delta-PE}(\mathbf{q}) = \sum_{i=1}^{\kappa} (m_i g)^2 (\Delta h_i)^2, \quad (6)$$

where $(m_i g)^2$ represents the weights, $(\Delta h_i)^2$ acts as the individual objective functions, and $\kappa = 6$ is the number of lumped masses.

2.3. Visual displacement

Visual displacement is defined as the absolute value of the site angle no matter where the target point is located. Therefore, minimizing visual displacement essentially minimizes the site angle. That is, the further the visual angle is from zero, the higher the value of the visual displacement function. This idea is formulated mathematically as what we call basic visual displacement:

$$VisualDisplacement = \theta(\mathbf{q})^2, \quad (7)$$

where the site angle θ is obtained using the arc cosine of the vector dot product. However, because of the arc cosine term necessary to find θ , Eq. (7) is discontinuous. To avoid this discontinuity, the following expression is proposed:

$$f_{VisualDisplacement}(\mathbf{q}) = n \left(1 - \cos \left[\frac{\theta(\mathbf{q})}{2} \right] \right), \quad (8)$$

where $n = 10$. This expression has the same basic conceptual significance and the same mathematical properties as Eq. (7) but avoids the discontinuities.

The MOO-based approach is different from traditional inverse kinematic methods or the experiment-based approach. It enforces human performance measures to drive the posture. One advantage of this approach is that one

just needs to add some additional constraints for different scenarios. For example, if the driver puts his/her elbow on the arm rest, to predict reaching posture one just adds another distance constraint between the elbow (another end-effector) and the arm rest to be zero. Another advantage is that this model is a generic one that can be easily extended to a model that considers all factors. We describe it as a generic model because any posture prediction for any scenario and any subject can be formulated as a MOO problem. One example is that this kinematic posture prediction model can be extended to include strength and body balance constraints.

3. Validation of Predicted Postures

In this section, we will describe the validation process, which includes validation tasks and participant selection, data collection using a motion capture system, experimental protocols, and the two-domain approach to validation.

3.1. Experiments

This study focuses on the in-car environment. We selected realistic in-vehicle tasks that test both the simple and the complex functionality of the human simulations. Figure 3 shows the four tasks that were chosen for the experiment. Task 1 requires reaching the point at the top of the A-pillar, a simple reach task. Task 2 requires reaching the radio tuner button, a slightly difficult reach task. Task 3 requires reaching the glove box handle, a difficult reach task. Task 4 requires reaching a point on the driver's B-pillar seatbelt adjuster. This is a complex task that requires reaching across the body and turning the head to see the target. The general procedure for achieving a task is as follows: the subject holds the steering wheel using both hands for the initial posture, then maintains the left handhold and uses the right index finger to touch the target point.

Good sampling is necessary to make sure that the anthropometric statistics resulting from a survey accurately represent the population of interest. To cover a larger driver population, auto designers choose a range of percentiles from 5% female to 95% male. Therefore, in our experiment, we chose four different populations, all Americans (Caucasians): 5th-percentile female, 50th-



Fig. 4. Experiment markers.

percentile female, 50th-percentile male, and 95th-percentile male. Three subjects were selected within each percentile, for a total of 12 participants. For males, the average height was 182.9 (SD 8.3) cm and the average mass was 90.7 (SD 14.4) kg. For females, the average height was 157.7 (SD 7.2) cm and the average mass was 58 (SD 5.9) kg. They were well distributed between the ages of 26 and 48 years. The protocol was approved by the Institutional Review Board of The University of Iowa. All participants gave informed consent prior to the study.

Optical systems have many applications in biomechanical studies.^{11,27,28} In the motion capture process, a number of reflective markers are attached over bony landmarks on the participant's body, such as the elbow, the clavicle, or the vertebral spinous processes. In this work, redundant markers (more than the minimum required) were used to compensate for occluded markers. The time history of the location of the reflective markers was collected using a Vicon motion capture system with eight cameras at a rate of 200 frames per second.

In the plug-in gait protocol, markers are attached to bony landmarks on the subject's body to establish local coordinate systems on various segments of the body. Joint centers and joint profiles can then be obtained using these coordinate systems. Methodologies for calculating joint center locations and link lengths of humans are available and have been somewhat successful.¹² In this work, due to the complexity of the capturing environment for a seated person inside a car and due to the limited number of cameras available at the time of the experiments (eight), redundant markers were attached to the upper part of the subject's body to estimate joint center locations and to compensate for the missing markers, as shown in Fig. 4. The marker placement protocol was designed to facilitate the process of obtaining the location of the joint centers of the upper part of the subject's body (right wrist, right elbow, right shoulder, and hip joint) during the experiments. In the marker placement protocol, one marker was attached to the end effector (the

end of the middle finger), three markers were attached to the wrist joint, and three markers were attached to the elbow joint. The shoulder joint is very complicated, so four markers were used to estimate the location of this joint center, and two markers were used to estimate the location of the clavicle (one on the clavicle and one on the T4).

3.2. Two-domain validation

In this study, we have developed a two-domain approach to validate the predicted posture.^{22,35} This approach validates the predicted posture in two domains: across percentiles and within percentiles. The weights for the objective function in Eq. (1) are chosen as $w_1 = 1.0$, $w_2 = 1.0$, and $w_3 = 0.01$ by the trail and error method. The first author's research group is investigating a systematic method (inverse optimization method) to determine weights within MOO cost functions.³⁸

3.2.1. Across percentiles. We have selected one representative subject for each percentile arbitrarily. That means there is one subject from each of the four different percentiles. Therefore, across percentiles we consider only four subjects and consider all tasks together. We first illustrate the coefficient of determination R^2 . Then, we only demonstrate the confidence intervals for the elbow joint angles. Figures 5(a) through 5(c) are regression plots of the Cartesian coordinates of x, y, and z for the joint centers of the right wrist, elbow, and shoulder, respectively. Figure 5(d) is the right elbow joint angle regression plot. The red straight line is at 45 degrees with respect to the X (horizontal) axis. All R^2 values satisfy $R^2 \geq 0.7$, and the slopes of all regressions are close to 1.

For confidence intervals, we demonstrate only the elbow joint angle in this paper; however, the procedure to determine the confidence intervals is the same as for other joint centers. The confidence interval of regression for the elbow joint angle with a 95% confidence level is $0.1115 \leq \rho^2 \leq 0.7967$ and is shown in Table I. The confidence interval for the slope of the regression of the elbow joint angle with a 95% confidence level is within (0.7033, 1.3038). The mean of elbow angle is -49.44 degrees and the confidence interval for mean with 95% confidence level is within (-65.58 , -33.30) degrees. The confidence interval of mean is shown in Fig. 6.

3.2.2. Within percentiles. In this category, we used a 50th-percentile male as one example to demonstrate the statistical validation results. All R^2 values satisfy $R^2 \geq 0.7$, except in the case of Shoulder x, which is shown in Fig. 7. The confidence intervals are straightforward, as in the examples above. In this case, the confidence interval of regression for the elbow joint angle (95% confidence level) is $0.4999 \leq \rho^2 \leq 0.9509$. The confidence interval for the slope of the regression of the elbow joint angle (95% confidence level) is within (1.075, 1.727). The mean value is -54.96 degrees and the confidence interval for mean with 95% confidence level is (-72.97 , -36.95) and is shown in Fig. 8.

In general, R^2 values are larger for across percentile case compared to within percentile case. According to statistic theory, larger R^2 value refers that the model is better. Actually this is not true. This is an indication that R^2 is not a perfect metric for model validation. Clustered x, y, or z will result in a larger R^2 , and an evenly spaced x, y, or z will result in a

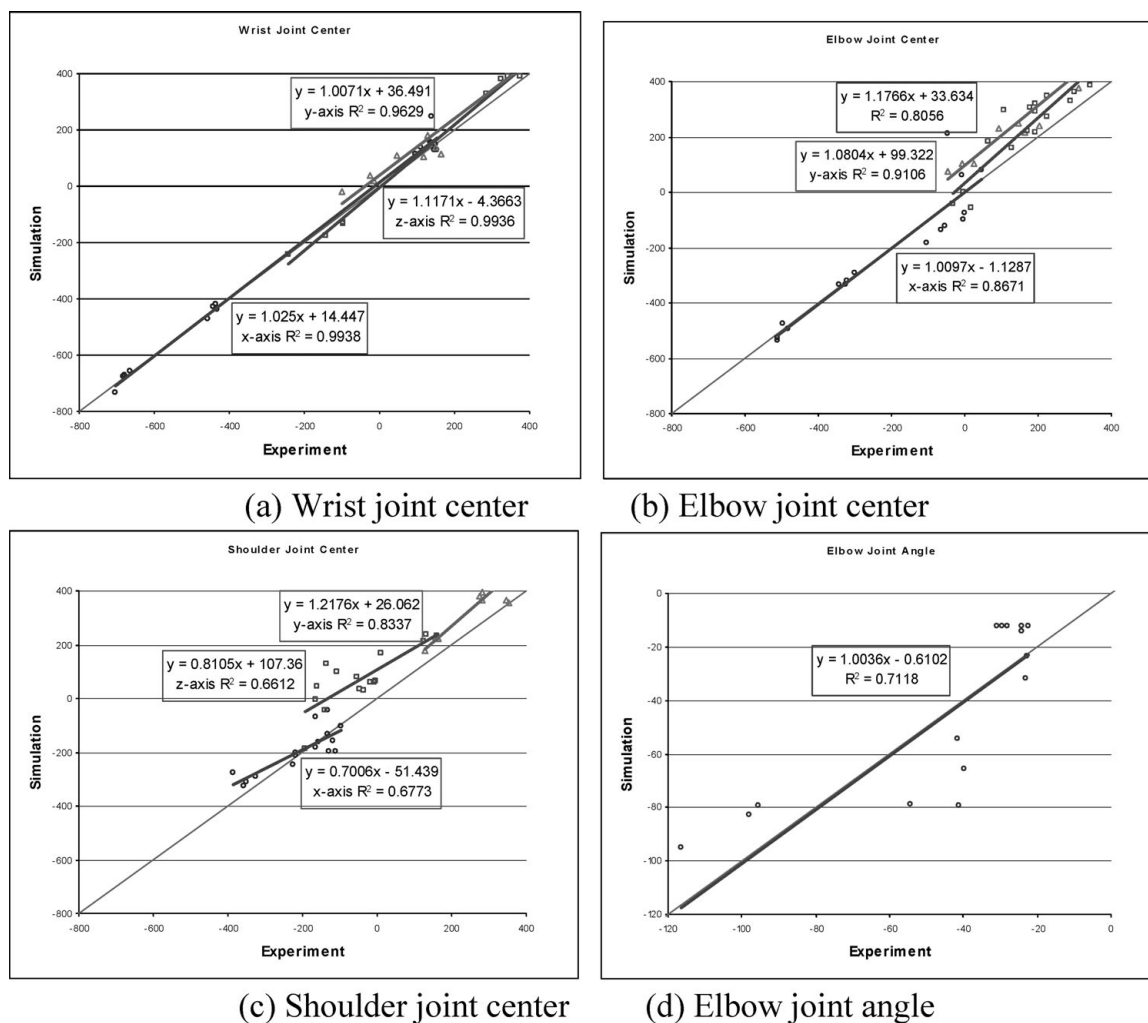


Fig. 5. Regression plots across percentiles.

Table I. Confidence interval of correlation.

Confidence intervals of correlation		95 % confidence levels		
Correlation coefficient R	0.7118			
z'	0.891			
z	1.960			
Standard error	0.27735			
Lower limit for z'	0.347217	ρ limits	0.333905	0.892571
Upper limit for z'	1.434429	ρ -squared	0.111493	0.796682

smaller R^2 . From Fig. 5 it is shown that the coordinates (x, y, and z) are clustered for across percentile case. Therefore, R^2 values are larger.

Figure 9 shows the snapshots of the simulation and experiment postures for one of the AM50 subjects. In general the simulated postures match approximately the experimental results well.

4. Conclusions and Discussions

This study presents a MOO-based posture prediction model and a systematical validation procedure. The MOO approach is a generic method in the sense that it can be adapted

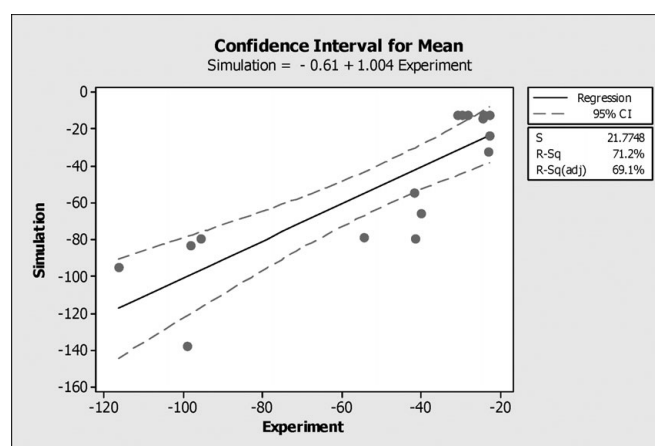
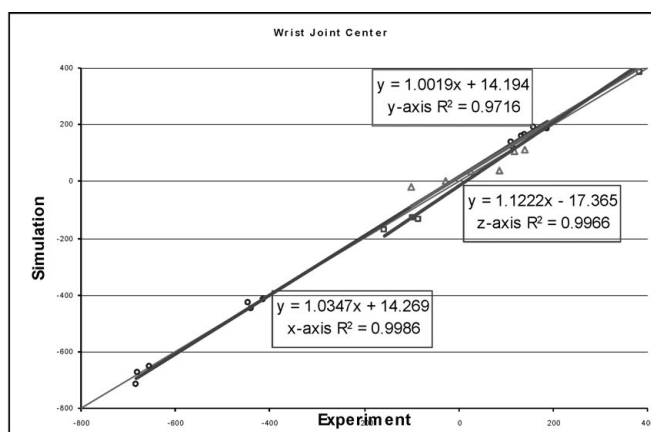
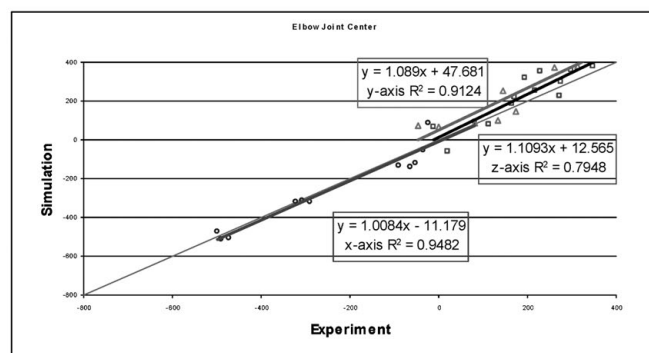


Fig. 6. Confidence interval for mean.

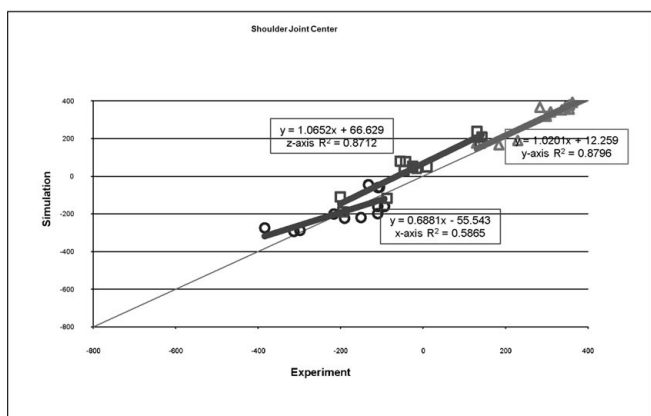
to any scenario and any subject including all different factors. In general, although there were errors from all different sources—such as the motion capture system, subject link lengths from measurement, the method that transforms markers on the skin to joint centers or joint angles, the human model, and the posture prediction model—the validation process was successful and the predicted postures were



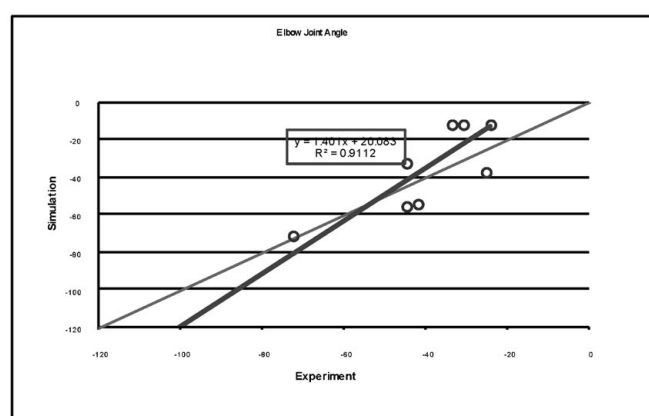
(a) Wrist joint center



(b) Elbow joint center



(c) Shoulder joint center



(d) Elbow joint angle

Fig. 7. Regression plots within male 50%.

within the required error limit. We used a two-domain approach to validate the predicted postures, and all plots contain a wealth of information. Generally, R^2 is a metric for the degree of precision of the model. The slope of the regression is another criterion to indicate the accuracy of the model. However, because we used a limited number of samples for validation, it was necessary to investigate confidence intervals to predict the range of values that was likely to indicate the unknown population.

In general, all R^2 are not less than 0.7 for the first two domains (within percentiles and across percentiles), all confidence intervals are reasonable, and they satisfy the validation requirement. However, most R^2 for the third domain (a specific task) are small. This phenomenon suggests that regression with respect to a task is not appropriate for validating the posture because it is a pure randomness problem.

Note that in the MOO posture prediction environment, the end-effector orientation constraint is available and it depends on the user to select it or not. In this paper, we did not discuss the orientation part because we did not validate the orientation.

This study also shows that we should consider the following aspects for the predicted posture and validation process:

- (1) There are several areas in which our model could be improved: (a) an advanced shoulder model considering

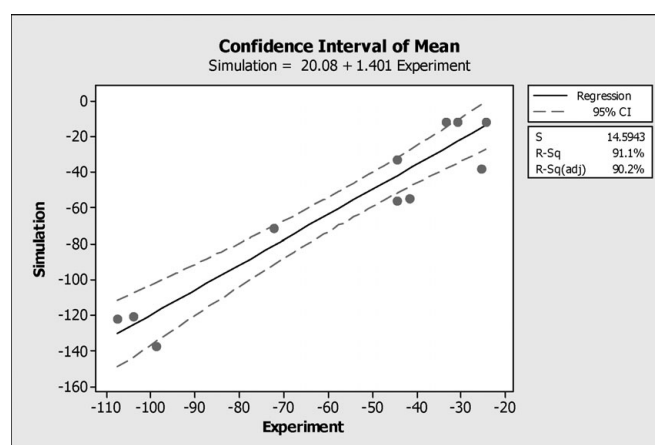


Fig. 8. Confidence interval of mean within male 50%.

scapula movement, coupled degrees of freedom, and coupled joint limits; (b) gender within the model; (c) hip movement; (d) neck and head model that is connected to the spine; (e) cognitive modeling aspects; and (f) bringing joint torque into the discomfort cost function.

- (2) A good sampling involves determining the sample size, as well as determining the sample structure in terms of age, gender, and race. In this study, we chose a sample size of 12. However, from the plots we have learned that

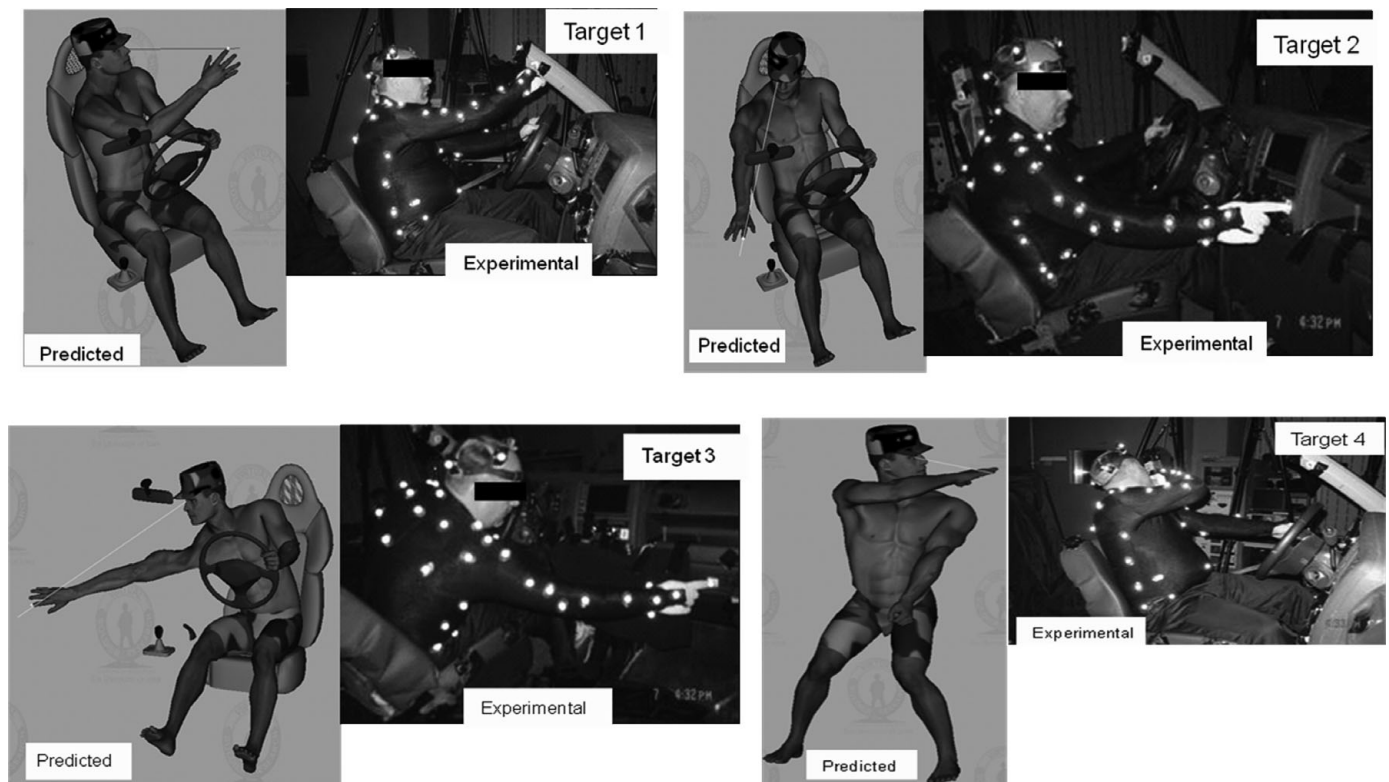


Fig. 9. Validation for four tasks.

we should increase the sample size to at least 40. Also, the age range was set at 26–48 years old. To accurately represent the population of interest for the vehicle interior design, we should increase the age range to include young drivers and seniors.

- (3) Weight sensitivity study is necessary for MOO-based posture prediction because weights play an important role indicating the relative importance of different human performance measures.
- (4) Boundary condition is one of the most important factors that affect the predicted posture where boundary condition defines how the human body interacts with the environment. For example, for the in-vehicle seated posture, the boundary condition entails collision avoidance between the body and the in-vehicle environment, including the seat, steering wheel, panel, ceiling, door, etc.
- (5) To extend this model to a dynamic environment, we have to include strength and balance constraints and external loads exerted in the hands and feet.

Acknowledgments

This work was partly supported by Caterpillar Inc., Honda R&D Americas Inc., and Texas Space Grant Consortium. The authors would like to thank anonymous reviewers for their valuable comments on earlier draft of this paper.

References

1. D. J. Beck and D. B. Chaffin, "An evaluation of inverse kinematics models for posture prediction," *In: Computer Applications in Ergonomics, Occupational Safety and Health* (M. Mattila and W. Karwowski, eds.) (Elsevier, Amsterdam, 1992) pp. 329–336.
2. J. C. Bean, D. B. Chaffin and A. B. Shultz, "Biomechanical model calculation of muscle contraction forces: A double linear programming method," *J. Biomech.* **21**, 59–66 (1988).
3. S. Byun, Development of a Multivariate Biomechanical Posture Prediction Model Using Inverse Kinematics *Ph.D. Dissertation* (Ann Arbor, MI: University of Michigan, 1991).
4. J. Denavit and R. S. Hartenberg, "A kinematic notation for lower-pair mechanisms based on matrices," *J. Appl. Mech.* **77**, 215–221 (1955).
5. B. Das and D. N. Behara, "Three-dimensional workspace for industrial workstations," *Hum. Factors* **40**(4), 633–646 (1998).
6. B. Das and A. K. Sengupta, "Computer-aided human modeling programs for workstation design," *Ergonomics* **38**, 1958–1972 (1995).
7. M. J. Dysart and J. C. Woldstad "Posture prediction for static sagittal-plane lifting," *J. Biomech.* **29**(10), 1393–1397 (1996).
8. J. J. Faraway, X. D. Zhang and D. B. Chaffin, "Rectifying postures reconstructed from joint angles to meet constraints," *J. Biomech.* **32**, 733–736 (1999).
9. P. Gill, W. Murray and A. Saunders, "SNOPT: An SQP algorithm for large-scale constrained optimization," *SIAM J. Optim.* **12**(4), 979–1006 (2002).
10. M. Griffin, "The validation of biodynamic models," *Clin. Biomech.* **16**(1), S81–S92 (2001).
11. K. Hagio, N. Sugano, T. Nishii, H. Miki, Y. Otake, A. Hattori, N. Suzuki, K. Yonenobu, H. Yoshikawa and T. Ochi, "A novel system of four-dimensional motion analysis after total hip arthroplasty," *J. Orthop. Res.* **22**(3), 665–670 (2004).
12. K. Halvorsen, M. Lesser and A. Lindberg, "A new method for estimating the axis of rotation and the center of rotation," *J. Biomech.* **32**, 1221–1227 (1999).
13. E. S. Jung, D. Kee and M. K. Chung, "Reach Posture Prediction of Upper Limb for Ergonomic Workspace Evaluation," *Proceedings of the 36th Annual Meeting of the Human Factors Society*, Atlanta, GA, Part 1, vol. 1 (1992), pp. 702–706.

14. E. S. Jung, D. Kee and M. K. Chung, "Upper body reach posture prediction for ergonomic evaluation models," *Int. J. Ind. Ergon.* **16**, 95–107 (1995).
15. E. S. Jung and J. Choe, "Human reach posture prediction based on psychophysical discomfort," *Int. J. Ind. Ergon.* **18**(2–3), 173–179 (1996).
16. D. Kee, E. S. Jung and S. Chang, "A man-machine interface model for ergonomic design," *Comput. Ind. Eng.* **27**, 365–368 (1994).
17. C. J. Kerk, Development and Evaluation of a Static Hand Force Exertion Capability Model Using Strength, Stability and Coefficient of Friction *Ph.D. Dissertation* (Ann Arbor, MI: University of Michigan, 1992).
18. J. Kim, J. Yang and K. Abdel-Malek, "Multi-objective optimization approach for predicting seated posture considering balance," *Int. J. Veh. Des.* **51**(3/4), 278–291 (2009).
19. Z. Mi, J. Yang and K. Abdel-Malek, "Optimization-based posture prediction for human upper body," *Robotica* **27**(4), 607–620 (2009).
20. R. T. Marler, S. Rahmatalla, M. Shanahan and K. Abdel-Malek, "A New Discomfort Function for Optimization-Based Posture Prediction," *Paper presented at the SAE Human Modeling for Design and Engineering Conference*, Iowa City, IA (June, 2005).
21. R. T. Marler, K. Farrell, J. Kim, S. Rahmatalla and K. Abdel-Malek, "Vision Performance Measures for Optimization-Based Posture Prediction," *Paper presented at the SAE Human Modeling for Design and Engineering Conference*, Lyon, France (July, 2006).
22. T. Marler, J. Yang, S. Rahmatalla, K. Abdel-Malek and C. Harrison, "New Validation Protocol for Predicted Posture," *Paper presented at the SAE Digital Human Modeling for Design and Engineering*, Seattle, University of Washington, WA (June 12–14, 2007).
23. R. T. Marler, J. S. Arora, J. Yang, H.-J. Kim and K. Abdel-Malek, "Use of multi-objective optimization for digital human posture prediction," *Eng. Optim.* **41**(10), 925–943 (2009).
24. K. S. Park, A Computerized Simulation Model of Postures during Manual Materials Handling *Ph.D. Dissertation* (Ann Arbor, MI: University of Michigan, 1973).
25. E. Pena Pitarch, J. Yang and K. Abdel-Malek, "Santos Hand: A 25-Degree-of-Freedom Model," *Paper presented at the SAE Digital Human Modeling for Design and Engineering*, Iowa City, IA (June 14–16, 2005).
26. J. M. Porter, K. Case and M. C. Bonney, "Computer Workspace Modeling," In: *Evaluation of Human Work* (J. R. Wilson and E. N. Corlett, eds.) (Taylor & Francis, London, 1990) pp. 472–499.
27. J. J. Robert, O. Michele and L. H. Gordon, "Validation of the Vicon 460 Motion Capture System for Whole-Body Vibration Acceleration Determination," *Paper presented at the ISB XXth Congress-ASB 29th Annual Meeting*, Cleveland, OH (Jul. 31–Aug. 5, 2005).
28. S. Rahmatalla, T. Xia, M. Contratto, D. Wilder, L. Frey-Law, G. Kopp and N. Grosland, "3D Displacement, Velocity, and Acceleration of Seated Operators in Whole-Body Vibration Environment using Optical Motion Capture Systems," *Paper presented at the Ninth International Symposium on the 3-D Analysis of Human Movement, Valenciennes (France)* (June 28–30, 2006).
29. D. Tolani, A. Goswami and N. Badler, "Real-time inverse kinematics techniques for anthropomorphic limbs," *Graph. Models* **62**(5), 353–388 (2000).
30. X. G. Wang and J. P. Verriest, "A geometric algorithm to predict the arm reach posture for computer-aided ergonomic evaluation," *J. Vis. Comput. Animat.* **9**, 33–47 (1998).
31. X. Wang, "A behavior-based inverse kinematics algorithm to predict arm prehension postures for computer-aided ergonomic evaluation," *J. Biomech.* **32**, 453–460 (1999).
32. X. Wang, N. Chevalet, G. Monnier, S. Ausejo, A. Suescun and J. Celigueta, "Validation of a Model-Based Motion Reconstruction Method Developed in the REALMAN Project," *Proceedings of SAE Digital Human Modeling for Design and Engineering Symposium*, Paper no. 2005-01-2743, Iowa City, IA (June 14–16, 2005).
33. J. Yang, R. T. Marler, H. Kim, J. Arora and K. Abdel-Malek, Multi-Objective Optimization for Upper Body Posture Prediction, *The 10th AIAA/ISSMO Multidisciplinary Analysis and Optimization Conference*, Albany, NY, (Aug. 30–Sep. 1, 2004).
34. J. Yang, T. Marler, H. J. Kim, K. Farrell, A. Mathai, S. Beck, K. Abdel-Malek, J. Arora and K. Nebel, "A New Generation of Virtual Humans," *SAE 2005 World Congress*, Cobo Center, Detroit, MI (Apr. 11–14, 2005).
35. J. Yang, S. Rahmatalla, T. Marler, K. Abdel-Malek and C. Harrison, "Validation of Predicted Posture for the Virtual Human Santos," *The 12th International Conference on Human-Computer Interaction (HCI)*, Beijing International Convention Center, Beijing, China (Jul. 22–27, 2007a).
36. J. Yang, R. T. Marler, S. Beck, K. Abdel-Malek and J. Kim, "Real-time optimal reach-posture prediction in a new interactive virtual environment," *J. Comput. Sci. Technol.* **21**(2), 189–198 (2006).
37. J. Yang, J. Kim, K. Abdel-Malek, T. Marler, S. Beck and G. Kopp, "A new digital human environment and assessment of vehicle interior design," *Comput.-Aided Des.* **39**, 548–558 (2007b).
38. Q. Zou, Q. Zhang and J. Yang, "Determining Weights of Joint Displacement Objective Function in Optimization-Based Posture Prediction," *First International Conference on Applied Digital Human Modeling*, Miami, FL (Jul. 17–20, 2010).